

The Measurement Of The Anomalous Magnetic Moment Of The Muon at Fermilab^a

I.Logashenko^{1,2,b}, J. Grange³, P. Winter³, R.M. Carey⁴, E. Hazen⁴, N. Kinnaird⁴, J.P. Miller⁴, J. Mott⁴, B.L. Roberts⁴, J. Crnkovic⁵, W.M. Morse⁵, H. Kamal Sayed⁵, V. Tishchenko⁵, V.P. Druzhinin^{1,2}, Y.M. Shatunov^{1,2}, R. Bjorkquist⁶, A. Chapelain⁶, N. Eggert⁶, A. Frankenthal⁶, L. Gibbons⁶, S. Kim⁶, A. Mikhailichenko⁶, Y. Orlov⁶, N. Rider⁶, D. Rubin⁶, D. Sweigart⁶, D. Allspach⁷, E. Barzi⁷, B. Casey⁷, M.E. Convery⁷, B. Drendel⁷, H. Freidsam⁷, C. Johnstone⁷, J. Johnstone⁷, B. Kiburg⁷, I. Kourbanis⁷, A.L. Lyon⁷, K.W. Merritt⁷, J.P. Morgan⁷, H. Nguyen⁷, J-F. Ostiguy⁷, A. Para⁷, C.C. Polly⁷, M. Popovic⁷, E. Ramberg⁷, M. Rominsky⁷, A.K. Soha⁷, D. Still⁷, T. Walton⁷, C. Yoshikawa⁷, K. Jungmann⁸, C.J.G. Onderwater⁸, P. Debevec⁹, S. Leo⁹, K. Pitts⁹, C. Schlesier⁹, A. Anastasi^{10,11}, D. Babusci¹⁰, G. Corradi¹⁰, S. Dabagov^{10,12}, C. Ferrari^{10,13}, A. Fioretti^{10,13}, C. Gabbanini^{10,13}, D. Hampai¹⁰, A. Palladino¹⁰, G. Venanzoni¹⁰, R. Di Stefano^{14,15}, M. Iacovacci^{14,16}, S. Marignetti^{14,15}, S. Mastroianni¹⁴, G. Di Sciascio¹⁷, D. Moricciani¹⁷, G. Cantatore^{18,19}, M. Karuza^{18,20}, K. Giovanetti²¹, V. Baranov²², V. Duginov²², N. Khomutov²², V. Krylov²², N. Kuchinskiy²², V. Volnykh²², M. Gaisser^{23,24}, S. Haciomeroglu^{23,24}, Y. Kim^{23,24}, S. Lee^{23,24}, M. Lee^{23,24}, Y. K. Semertzidis^{23,24}, E. Won^{23,25}, R. Fatemi²⁶, W. Gohn²⁶, T. Gorringer²⁶, T. Bowcock²⁷, J. Carroll²⁷, B. King²⁷, S. Maxfield²⁷, A. Smith²⁷, T. Teubner²⁷, M. Whitley²⁷, A. Wolski^{27,28}, M. Wormald²⁷, S. Al-Kilani²⁹, R. Chislett²⁹, M. Lancaster²⁹, E. Motuk²⁹, T. Stuttard²⁹, M. Warren²⁹, D. Flay³⁰, D. Kwall³⁰, Z. Meadows³⁰, M. Syphers³¹, D. Tarazona³¹, T. Chupp³², A. Tewlsey-Booth³², B. Quinn³³, M. Eads³⁴, A. Epps³⁴, G. Luo³⁴, M. McEvoy³⁴, N. Pohlman³⁴, M. Shenk³⁴, A. de Gouvea³⁵, H. Schellman^{35,36}, L. Welty-Rieger³⁵, B. Abi³⁷, F. Azfar³⁷, S. Henry³⁷, F. Gray³⁸, C. Fu³⁹, X. Ji³⁹, L. Li³⁹, H. Yang³⁹, D. Stockinger⁴⁰, D. Cauz^{41,42}, G. Pauletta^{41,42}, L. Santi^{41,42}, S. Baessler^{43,44}, E. Frlez⁴³, D. Pocanic⁴³, L. P. Alonzi⁴⁵, M. Ferti⁴⁵, A. Fienberg⁴⁵, N. Froemming⁴⁵, A. Garcia⁴⁵, D. W. Hertzog⁴⁵, P. Kammel⁴⁵, J. Kaspar⁴⁵, R. Osofsky⁴⁵, M. Smith⁴⁵, E. Swanson⁴⁵, K. Lynch⁴⁶

¹*Budker Institute of Nuclear Physics, Novosibirsk, 630090, Russia*

²*Novosibirsk State University, Novosibirsk, 630090, Russia*

³*Argonne National Laboratory, Lemont, IL, USA*

^aContributed paper, published as part of the Proceedings of the Fundamental Constants Meeting, Eltville, Germany, February 2015.

^b Author to whom correspondence should be addressed. Electronic mail: I.B.Logashenko@inp.nsk.su.

- ⁴*Boston University, Boston, MA, USA*
- ⁵*Brookhaven National Laboratory, Upton, NY, USA*
- ⁶*Cornell University, Ithaca, NY, USA*
- ⁷*Fermi National Accelerator Laboratory, Batavia, IL, USA*
- ⁸*University of Groningen, KVI, Groningen, The Netherlands*
- ⁹*University of Illinois at Urbana-Champaign, Urbana, IL, USA*
- ¹⁰*Laboratori Nazionali di Frascati dell'INFN, Frascati, Italy*
- ¹¹*Dipartimento di Fisica e di Scienze della Terra dell'Università di Messina, Messina, Italy*
- ¹²*Lebedev Physical Institute and NRNU MEPhI, Moscow, Russia*
- ¹³*Istituto Nazionale di Ottica, UOS Pisa, Consiglio Nazionale delle Ricerche, Italy*
- ¹⁴*Istituto Nazionale di Fisica Nucleare, Sezione di Napoli, Napoli, Italy*
- ¹⁵*Università di Cassino, Cassino, Italy*
- ¹⁶*Università di Napoli, Napoli, Italy*
- ¹⁷*Istituto Nazionale di Fisica Nucleare, Sezione di Roma Tor Vergata, Roma, Italy*
- ¹⁸*Istituto Nazionale di Fisica Nucleare, Sezione di Trieste, Trieste, Italy*
- ¹⁹*Università di Trieste, Trieste, Italy*
- ²⁰*University of Rijeka, Rijeka, Croatia*
- ²¹*James Madison University, Harrisonburg, VA, USA*
- ²²*Joint Institute for Nuclear Research, Dubna, Russia*
- ²³*KAIST, Daejeon, Republic of Korea*
- ²⁴*Center for Axion and Precision Physics (CAPP) / Institute for Basic Science (IBS), Daejeon, Republic of Korea*
- ²⁵*Korea University, Seoul, Republic of Korea*
- ²⁶*University of Kentucky, Lexington, KY, USA*
- ²⁷*University of Liverpool, Liverpool, United Kingdom*
- ²⁸*The Cockcroft Institute, Daresbury, United Kingdom*
- ²⁹*University of College London, London, United Kingdom*
- ³⁰*University of Massachusetts, Amherst, MA, USA*
- ³¹*Michigan State University, East Lansing, MI, USA*
- ³²*University of Michigan, Ann Arbor, MI, USA*
- ³³*University of Mississippi, Oxford, MS, United States*
- ³⁴*Northern Illinois University, DeKalb, IL, USA*
- ³⁵*Northwestern University, Evanston, IL, USA*
- ³⁶*Oregon State University, Corvallis, OR, United States*
- ³⁷*University of Oxford, Oxford, United Kingdom*
- ³⁸*Regis University, Denver, CO, USA*
- ³⁹*Shanghai Jiao Tong University, Shanghai, China*
- ⁴⁰*Technische Universität Dresden, Dresden, Germany*
- ⁴¹*Università di Udine, Udine, Italy*

⁴²*INFN, Sezione di Trieste, Trieste, Italy*

⁴³*University of Virginia, Charlottesville, VA, USA*

⁴⁴*Oak Ridge National Laboratory, Oak Ridge, TN, United States*

⁴⁵*University of Washington, Seattle, WA, USA*

⁴⁶*York College, CUNY, Jamaica, NY, USA*

The anomalous magnetic moment of the muon is one of the most precisely measured quantities in experimental particle physics. Its latest measurement at Brookhaven National Laboratory deviates from the Standard Model expectation by approximately 3.5 standard deviations. The goal of the new experiment, E989, now under construction at Fermilab, is a 4-fold improvement in precision. Here we discuss the details of the future measurement and its current status.

Key words: Standard Model, anomalous magnetic moment

1. Introduction

The Standard Model is an exceptionally successful theory, able to explain practically all experimental results in the field of particle physics. Nevertheless, there are observations which tell us that it is incomplete: the model parameters have to be exceptionally fine-tuned, astrophysical observations require the existence of “dark matter” and “dark energy”, etc. At the energy frontier searches for physics beyond SM are principally being performed at the LHC, but so far no convincing evidence of a SM violation has been found. A precise measurement of the anomalous magnetic moment of the muon provides a complementary search for new physics..

The gyromagnetic factor, g , relates the intrinsic magnetic moment $\vec{\mu}$ of charged particle with its spin \vec{s} . The Dirac theory predicts $g = 2$ for point-like spin-1/2 particles. However, in the framework of QFT, the higher order effects modify the value of g . The deviation of the gyromagnetic factor from 2, $a = (g - 2)/2$, is called the anomalous magnetic moment. All existing fields make contributions to a , potentially even those, which were never observed at colliders. The heavier the virtual particles, or the smaller the coupling constant, the smaller the corresponding contribution to a . The dominant contribution to a comes from QED, described in the lowest order by the Schwinger term $\alpha/2\pi \approx 10^{-3}$. The unique feature of the anomalous magnetic moment of the muon, a_μ , is its relatively high sensitivity to non-QED fields. In general, the contribution to the anomalous magnetic moment of a particle with mass m from a massive field with mass m_X scales as $\sim (m_X/m)^2$. Thus non-QED contributions (including potential contributions from New Physics) to a_μ are about $(m_\mu/m_e)^2 \approx 40000$ larger than the same

contribution to a_e . The anomalous magnetic moment of the tau lepton would be even more sensitive, but its short lifetime makes a precision measurement impossible.

The measurement of a_μ has a long, more than 50 year history. The series of measurements, started in the 1950s first at the Nevis cyclotron and then at CERN where the non-zero value of the anomaly was confirmed, and then the importance of the contributions from the higher-order QED and virtual hadrons was shown. The latest measurement by the E821 experiment¹ at the Brookhaven National Laboratory, which completed data taking in 2001, was the first to be sensitive to contributions from all known fields – QED, QCD and electroweak (EW). The 0.54 ppm precision of the a_μ measurement is well matched by the 0.42 ppm precision of the Standard Model prediction². This state-of-the-art calculation takes into account QED contribution up to five loops and hadronic and electroweak contributions up to leading and next-to-leading order. The comparison between the measured and SM values of a_μ is shown in Table 1. An extremely interesting result of the BNL experiment is that the measured value is $2.2 \div 2.5$ ppm, or $3.3 \div 3.6$ standard deviations above the SM expectation. While this difference is below the commonly accepted discovery threshold of 5σ , it prompted a wide interest in a more precise measurement and calculation of a_μ and speculations about possible new physics contribution.

TABLE 1. Summary of the Standard Model evaluation of a_μ and the comparison with the Brookhaven result. Two values are quoted for the lowest-order hadronic contribution HVP (lo), following the two recent evaluations.

	Value ($\times 10^{-11}$) units
QED	$116\,584\,718.951 \pm 0.009 \pm 0.019 \pm 0.007 \pm 0.077$
HVP (lo) ³	$6\,923 \pm 42$
HVP (lo) ⁴	$6\,949 \pm 43$
HVP (ho)	-98.4 ± 0.7
LbL	105 ± 26
EW	153.6 ± 1.0
Total SM ³	$116\,591\,802 \pm 42_{H-LO} \pm 26_{H-HO} \pm 2_{other} (\pm 49_{tot})$
Total SM ⁴	$116\,591\,828 \pm 43_{H-LO} \pm 26_{H-HO} \pm 2_{other} (\pm 50_{tot})$
E821	$116\,592\,089 \pm 63$ (0.54 ppm)
$\Delta a_\mu(\text{E821-SM})^3$	287 ± 80
$\Delta a_\mu(\text{E821-SM})^4$	261 ± 80

A new Muon g-2 experiment, E989⁵, now under construction at Fermilab, aims to measure a_μ to a precision of 0.14 ppm: a factor of 4 improvement over the BNL result. In the following sections, the features of the new experiment making this improvement possible will be discussed. Expectation of a more precise measurement of a_μ have triggered a world-wide effort to improve the accuracy of the SM prediction. The uncertainty of $a_\mu(\text{SM})$ is dominated by the hadronic contribution. Due to the non-perturbative nature of QCD, one cannot apply perturbative techniques, used to evaluate the QED and EW contributions, to calculate the hadronic contribution. The lowest order hadronic contribution HVP (lo) is calculated through the dispersion relation

$$a_{\mu}^{had;LO} = \left(\frac{\alpha m_{\mu}}{3\pi}\right)^2 \int_{m_{\pi}^2}^{\infty} \frac{ds}{s^2} K(s) R(s), \text{ where } R = \frac{\sigma_{tot}(e^+e^- \rightarrow hadrons)}{\sigma(e^+e^- \rightarrow \mu^+\mu^-)}. \quad (1)$$

This calculation uses the measured cross sections for $e^+e^- \rightarrow hadrons$ as an input. It turns out, that the dominant contribution to the value of the integral and to its error comes from the low energies $\sqrt{s} \lesssim 2$ GeV. A number of new measurements of $e^+e^- \rightarrow hadrons$ have appeared over the last decade from the CMD-2 and SND experiments at Novosibirsk, the KLOE experiment at Frascati and the BaBar experiment at SLAC. Several experiments: CMD-3 and SND at Novosibirsk and BES-III at Beijing aim to provide new, more precise data on $e^+e^- \rightarrow hadrons$ over the next few years. Another part of the hadronic contribution, the light-by-light (LbL) contribution $a_{\mu}^{had;LbL}$, cannot at present be determined from the data and its calculation is intrinsically model-dependent. The current estimation of its uncertainty takes into account the difference between the models. Evaluation of the light-by-light hadronic contribution is an active field of research. There are efforts to improve the models using the transition form factors measured in experiment, and to calculate $a_{\mu}^{had;LbL}$ in the framework of lattice QCD. With all this world-wide effort, one can expect that the unprecedented precision of E989 will be matched by a 20%-50% improvement in the accuracy of the Standard Model prediction.

2. Experimental technique

The basic layout of the experiment dates back to the third CERN experiment⁶ with a number of improvements introduced at Brookhaven (most notably, the muon injection). A short bunch of protons hits a target and the pions produced at the target are collected and steered to a long beam line where they decay into muons. In the pion decay $\pi^+ \rightarrow \mu^+ \nu_{\mu}$, the direction of the muon spin is 100% correlated to the direction of the muon momentum in the rest frame of the pion. Therefore, selecting the highest-energy muons in the lab frame, one can achieve a muon beam polarization of 90% or more. The polarized muons are injected into the storage ring with an ultra-uniform magnetic field, where they stay on a circular orbit with a cyclotron frequency ω_c . The muon spin rotates in the same field with frequency ω_s . The precession of the muon spin relative to the direction of muon momentum in the presence of electric and magnetic fields is

$$\omega_a = \omega_s - \omega_c = \frac{e}{m} \left(a_{\mu} B - \left[a_{\mu} - \frac{1}{\gamma^2 - 1} \right] \frac{|\vec{\beta} \times \vec{E}|}{c} \right) \quad (2)$$

The muon beam would quickly spread out vertically in the uniform magnetic field due to its intrinsic momentum and angular spread. The standard solution: the introduction of a gradient to the B field, would lead to a large sensitivity of the experiment to beam dynamics. Fortunately, with a particular choice of “magic” $\gamma \approx 29.3$ ($p_{\mu} = 3.1$ GeV), the second term vanishes and the precession frequency becomes independent of the focusing quadrupole field E:

$$\omega_a = a_\mu \frac{eB}{m} \quad (3)$$

Thus, the measurement of a_μ is reduced to high-precision measurement of the magnetic field B and the precession frequency ω_a . The static electric quadrupoles are used to store the muon beam vertically in the ultra-uniform magnetic field. To first order, the presence of the electric field does not affect the precession frequency (in the second order, a small well-calculated 1 ppm-level correction occurs due to the presence of the momentum spread). The choice of the “magic” γ determines the size of experiment: the E821 storage ring had a 7.1 m radius and a 1.45 T magnetic field.

The E821 experiment was statistics limited. The E989 experiment aims for a 20-fold increase in statistics in about 1-2 years of data taking. The Fermilab accelerator complex has unique features to make this increase possible. The E989 experiment makes use of equipment from the now decommissioned antiproton source: target, lithium lens, magnets from the former Antiproton accumulator and the Debuncher ring, etc. The particle flow is as follows. A burst of $4 \cdot 10^{12}$ protons with a kinetic energy of 8 GeV are injected into the Recycler ring where they are regrouped into 4 bunches. Each bunch is extracted one-at-a-time and sent to the pion production target. Particles with momentum 3.11 GeV/c ($\pm 10\%$) are sent to the 270 m beam line, where most pions decay. At the end of the line, particles with momentum 3.094 GeV/c are selected and sent to the Delivery ring (part of the former antiproton source), where they are stored for 3-5 turns. This 2 km path allows nearly all pions to decay and also introduces a time separation between the muons and the remaining protons. Then the pure muon beam is injected into the muon storage ring. Compared to E821, the E989 muon source is both purer and more intense.

The core piece of experiment is the muon storage ring magnet (Fig.1). The magnet yoke is made up 12 azimuthal sections, each of which consists of six layers of high quality magnet steel. The ultra-uniform field in the storage volume is shaped by the pole pieces and a set of shims. The magnetic field is created by large superconducting coils of about 7.1 m radius. E989 reuses the E821 storage ring magnet. The yoke was disassembled at BNL and all the pieces were transported to Fermilab. The challenging task of moving the three large and fragile superconducting coils was successfully achieved in 2013. In 2014 the E989 experimental hall was constructed and the ring was assembled back. The photo of the E821 storage ring magnet partially assembled in the E989 hall at Fermilab is shown in Fig. 2.

In addition to the increase of statistics, a number of upgrades will be introduced in E989, aimed at reducing the systematic error. Table 2 shows the systematic and statistical uncertainties for the E821 and projections for E989. In the following sections we briefly described the expected improvements of the experimental techniques.

TABLE 2. Systematic and statistical uncertainties for the Brookhaven muon g-2 measurement and the projections for the Fermilab experiment. The uncertainties are given in parts-per-billion (ppb).

Uncertainty source	BNL (ppb)	FNAL goal (ppb)
Statistics	480	100
Measurement of precession frequency	180	70
Measurement of magnetic field	170	70
Total	540	140

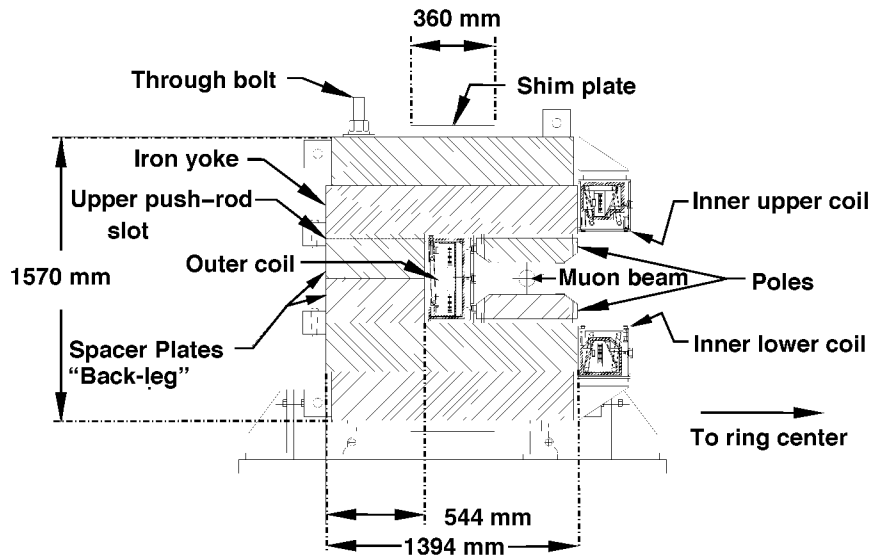


FIG. 1. Cross section of the muon storage ring magnet.

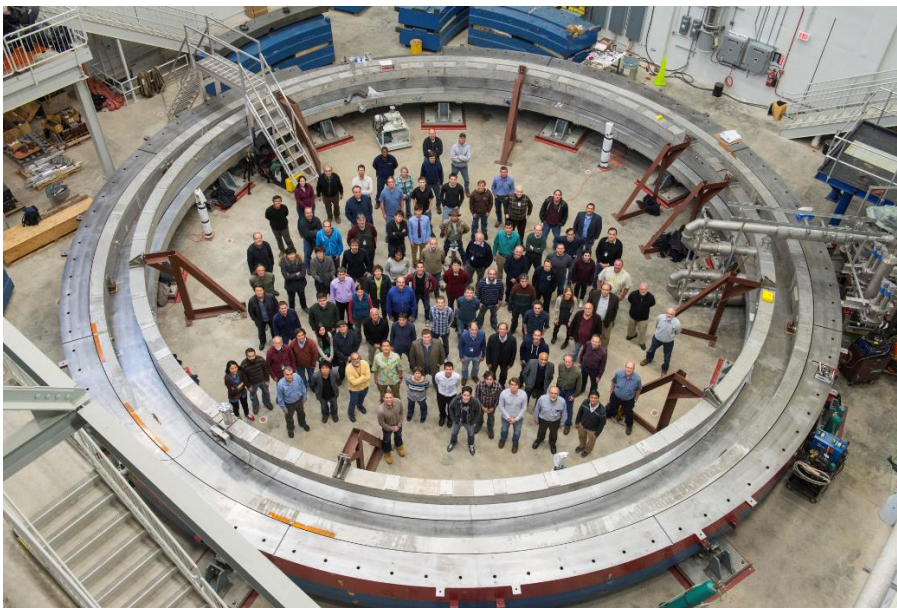


FIG 2. Muon storage ring assembled in E989 experimental hall (Nov.2014). Lower part of the yoke and superconducting coils are visible.

3. Measurement of the magnetic field

The magnetic field B in (3) is an average field seen by the stored muons. In order to reduce the sensitivity of the measurement from the beam dynamics and the muon momentum spread, it is important to have a homogeneous field in both the longitudinal and transverse directions. This is achieved by a large set of shimming tools. At E821, a uniformity of better than 1 ppm over the storage volume for the average field seen by the muons was achieved.

The magnetic field is measured in terms of the NMR frequency of the free proton ω_p . Intrinsically, the NMR technique allows one to measure the field to ~ 20 ppb, well within E989 requirements. But the diamagnetic shielding inside the sample volume introduce systematic shifts of a few 10^3 's of ppm, two orders of magnitude larger the E989 requirements. Thus, a precise calibration chain is required to carefully account for all systematic effects.

The absolute calibration utilizes a probe with a spherical water sample⁷. The same technique was used at E821, but with the improvements of the original probe design and the development of an alternative ^3He -based probe, E989 aims to improve the accuracy of the absolute calibration from 50 ppb (E821) to 35 ppb. With the help of the special “plunging” probe, which can be moved to the storage region in vacuum, the absolute calibration is transferred to 17 cylindrical NMR probes, installed on the trolley. Every few days, the trolley runs around the ring in vacuum and maps the field in the storage region. Collections of 378 fixed NMR probes, positioned above and below the vacuum chamber, provide the continuous monitoring of the field between the trolley runs, when the beam is in the storage ring. A number of upgrades of this calibration chain were proposed for E989, which include better positioning of the probes, better temperature stabilization, more frequent measurements, etc. With all these improvements, E989 aims to reach a 70 ppb systematic error for ω_p (the best result, achieved at E821, was 170 ppb).

Equation (3) can be rewritten to directly use ω_p and ω_a :

$$a_\mu = \frac{\omega_a/\omega_p}{\mu_{\mu^+}/\mu_p - \omega_a/\omega_p} \quad (4)$$

where $\mu_{\mu^+}/\mu_p = 3.183\,345\,24(37)$ was determined from the E1054 LAMPF measurement of Zeeman ground state hyperfine transition in muonium^{8,9}. The 120 ppb precision of μ_{μ^+}/μ_p nearly equals the expected 140 ppb accuracy of ω_a/ω_p , which reduces the final precision of a_μ . The ratio μ_{μ^+}/μ_p can be independently determined 5 times more precisely from the relation:

$$\frac{\mu_\mu}{\mu_p} = \frac{m_e \mu_e g_\mu}{m_\mu \mu_p g_e} \quad (5)$$

where m_e/m_μ is known to 25 ppb, μ_e/μ_p is known to 8.1 ppb and g_μ/g_e to better than 1 ppb⁸. In this approach, since m_e/m_μ is obtained from the hyperfine structure of muonium using the SM prediction, then any beyond-the-SM theory being tested against the measured value of a_μ should have the BSM contribution to m_e/m_μ taken into account.

4. Measurement of the precession frequency

In the weak decay of the muon $\mu \rightarrow e\nu\bar{\nu}$, there is correlation between the direction of the emitted electron and the direction of the muon spin in the muon rest frame. In addition, this correlation is dependent on the electron energy and it is at its maximum for the highest energies. Translated to the lab frame, this correlation manifests itself in a variation of the energy spectrum for the decay positrons: there are more high energy positrons when the muon spin and momentum are aligned. This property of the muon decay is exploited for ω_a measurement. The decay positrons are detected by 24 PbF₂ calorimeters placed on the inner part of the storage ring. The rate of detected positrons above a single energy threshold E_{thr} (typically, 1.8 GeV) is

$$\frac{dN}{dt} = N_0 e^{-t/\gamma\tau_\mu} [1 + A \cos(\omega_a t + \varphi)] \quad (6)$$

where the normalization N_0 , asymmetry A and initial phase φ depend on E_{thr} . In the first approximation, ω_a is determined by fitting the measured time distribution dN/dt by a simple 5-parameter function (6), as illustrated in Fig. 3. But there are additional effects which modify (6). The most important of them are listed below.

1. Pileup. Two positrons can simultaneously hit the calorimeter and be misreconstructed as single positron. This coincidence-based effect introduces a $2\omega_a$ terms in dN/dt . A number of E989 features will mitigate the pileup contribution. While the average beam intensity in E989 is higher than in E821, the instantaneous rate is about the same, which allows the number of coincidences to be kept at a similar level. The E989 calorimeters are segmented, which allows one to reduce pileup by reconstructing spatially-separated positrons. The specially designed thresholdless electronics allows not only to count positrons above given threshold, but also to measure dE/dt – the total deposited energy as a function of time. This quantity also follows (6), with a somewhat smaller asymmetry, and it is unaffected by pileup. A simultaneous measurement of ω_a by the analysis of dN/dt and dE/dt will provide an important systematics test. Overall, E989 aims to reduce the pileup contribution uncertainty to 40 ppb from 80 ppb at E821.
2. Coherent betatron oscillations (CBO). In a weak focusing ring, the beam position and spread has periodic movements with a frequency ω_{CBO} . This variation of the beam position, coupled with the non-uniform acceptance of the detectors and other effects, lead to an additional decaying oscillation term for the normalization N_0 , asymmetry A and initial phase φ in (6) with the frequency ω_{CBO} . In E821 this systematic effect was enhanced for two reasons: the muon beam

was underkicked at injection, which increases the amplitude of the CBO; and for a significant part of the data ω_{CBO} was quite close to $2\omega_a$. The proposed E989 upgrades, such as the use new muon kicker and the improved electrostatic quadrupoles with stronger focusing (which will move ω_{CBO} further away from $2\omega_a$), will bring the CBO contribution to the systematic uncertainty to below 30 ppb from 70 ppb at E821.

3. Gain changes. After injection, the muon beam is observed by the calorimeters for about 10 muon lifetimes ($\approx 700 \mu\text{s}$). Thus over a period of 1 ms the instantaneous rate at the calorimeters changes by 4 orders of magnitude. Any rate-dependence of the calorimeter response would introduce a large systematic effect on ω_a . The calorimeter readout and electronics are designed to meet this requirement. A state-of-the-art laser calibration system with high stability will continuously monitor the calorimeters' performance. With all these improvements, E989 plans to reduce the systematic error due to gain changes to 20 ppb from 120 ppb at E821.

An important part of the E989 instrumentation are the nearly massless tracking chambers, placed in vacuum upstream of three calorimeter stations. These chambers record the positron track before it hits the calorimeter and provide data-based constraints on beam-related systematic uncertainties and pileup. These chambers are also the primary detectors for the measurement of the electric dipole moment of muon, which will be done simultaneously with the measurement of a_μ .

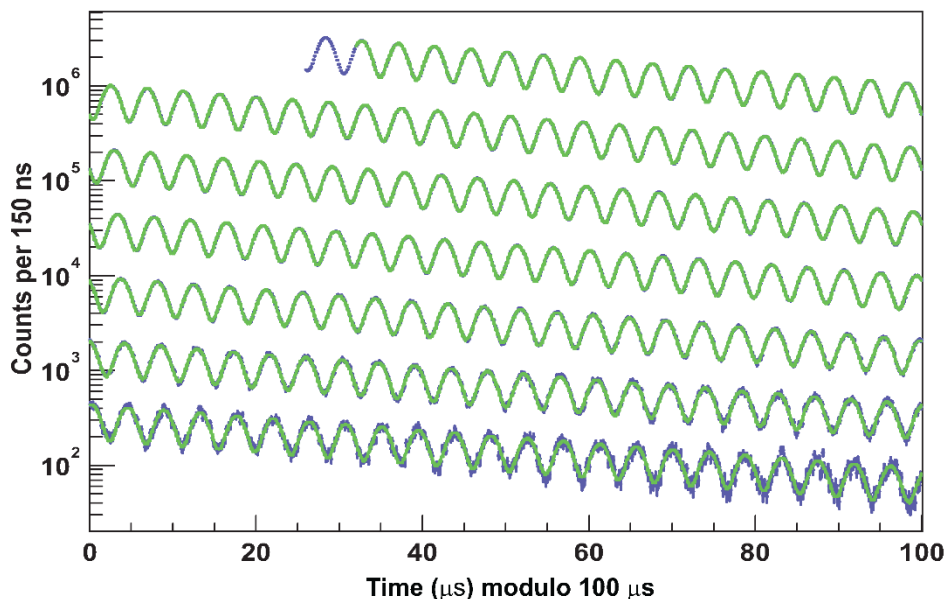


FIG. 3. Histogram, modulo $100 \mu\text{s}$, of the number of detected decay electrons above 1.8 GeV for the E821 2001 data as a function of time, with a fit superimposed. Total statistics is 3.6×10^9 electrons.

5. Conclusion

The deviation between the value of the anomalous magnetic moment of the muon and its SM prediction, observed by the BNL E821 experiment, is one of the most prominent hints of physics beyond the SM. The goal of the new E989 experiment

at Fermilab is a 4-fold improvement in the precision of a_μ measurement. If the observed deviation is indeed a manifestation of the New Physics, the new measurement will prove it to more than a 5σ significance. If the new result does not confirm the deviation, it will serve as a powerful constraint for many beyond the SM models.

The E821 experiment was statistics limited. The unique features of the Fermilab accelerator complex will produce 20 times more statistics for the new measurement and while the E989 experiment is based on E821, the numerous upgrades will reduce the systematic error by a factor of three.

The E989 experiment is scheduled to begin data taking in early 2017.

References

- ¹Bennett, G.W. *et al.* (Muon g-2 Collaboration), Phys.Rev. D73 (2006) 072003.
- ²T. Blum, A. Denig, I. Logashenko, E. de Rafael, B. Lee Roberts, T. Teubner and G. Venanzoni, arXiv:1311.2198 [hep-ph].
- ³M. Davier, A. Hoecker, B. Malaescu and Z. Zhang, Eur. Phys. J. **C71** (2011) 1515, Erratum-ibid. **C72** (2012) 1874.
- ⁴K. Hagiwara, R. Liao, A. D. Martin, D. Nomura and T. Teubner, J. Phys. **G38** (2011) 085003.
- ⁵J. Grange *et al.* (Muon g-2 Collaboration), arXiv:1501.06858 [physics.ins-det].
- ⁶Bailey J. *et al.*, Nucl. Phys. B150 (1979) 1.
- ⁷X. Fei, V.W. Hughes and R. Prigl, Nucl.Instrum.Meth. **A394** (1997) 349-356.
- ⁸P. J. Mohr, B. N. Taylor and D. B. Newell, Rev. Mod. Phys. **84** (4) 1527 (2012).
- ⁹W. Liu *et al.*, Phys. Rev. Lett. **82** (1999) 711.